Nat. Hazards Earth Syst. Sci. Discuss., 2, 4069–4100, 2014
www.nat-hazards-earth-syst-sci-discuss.net/2/4069/2014/
doi:10.5194/nhessd-2-4069-2014

Natural Hazards and Earth System Sciences
Open Access
Discussions

Estimation of successive co-seismic vertical offsets using coeval sedimentary events – application to the Sea of Marmara's Central Basin (North Anatolian Fault)

C. Beck[1], C. Campos[1,2], K. Eriş[3], N. Çağatay[4], B. Mercier de Lepinay[5], and F. Jouanne[1]

[1]Laboratoire ISTerre, UMR CNRS 5275, Université de Savoie/Grenoble-Alpes University, 73 376 Le Bourget du Lac, France
[2]Departamento de Ciencias de la Tierra, Universidad Simón Bolívar, Sartenejas, Baruta, Venezuela
[3]Firat University Faculty of Engineering Geology Department, 23100, Elazığ, Turkey
[4]Istanbul Technical University EMCOL, 34469, Faculty of Mining Ayazağa, Ýstanbul, Turkey
[5]Geoazur, U.M.R. C.N.R.S 6526, Université de Nice-Sophia-Antipolis, 06560 Valbonne, France

Received: 27 January 2014 – Accepted: 24 February 2014 – Published: 6 June 2014

Correspondence to: C. Beck (beck@univ-savoie.fr)

Published by Copernicus Publications on behalf of the European Geosciences Union.

NHESSD
2, 4069–4100, 2014

Abstract

In the deep part of the Sea of Marmara (Turkey), the sedimentation developing upon the North Anatolian Fault is strongly influenced by the associated seismic activity. Specific layers (homogenites-turbidites), representing individual sedimentary events, have been characterized along three giant piston cores retrieved from Çinarcik and Central (or Orta) basins. Analyzed sediments represent the last 12 to 17 kyr BP. For a 2 kyr-lasting interval, 11 events could be precisely correlated on both sides of the Central Basin's southern scarp. For each of them, based on the specific depositional process, the thickness difference between the two sites was considered as a direct estimation of the vertical component of a coeval co-seismic offset. The homogenite (upper) term accounts for the major part of the thickness difference. The 6 most significant values range from 36 cm to 144 cm and are likely representing dominantly normal throws, with estimated paleomagnitudes (M_w) ranging from 5.9 to 6.6.

1 Introduction

Since several decades, sedimentary archives, either marine or lacustrine, have been explored as potential paleoseismic records, beside previously well-developed onland approaches (in McCalpin, 2009). For the subaqueous records, two major groups of effects can be detected and analyzed: (i) in situ post-depositional disturbances (e.g.: Marco and Agnon, 1995; Ken-Tor et al., 2001; Rodriguez-Pascua et al., 2002, 2003), (ii) gravity-driven reworking and re-settling of large masses of unconsolidated sediments (e.g.: Adams, 1990; Strasser et al., 2006).

Two major questions arise for both groups: (1) how to ensure the earthquake-triggering, (2) how to identify the responsible active structure(s). For in situ disturbances, the first problem is generally solved; in particular, it benefits from analogical and/or numerical modelling (e.g. Moretti et al., 1999; Wetzler et al., 2010). For redepositional processes – which are envisaged in the present work – several recent catas-

NHESSD

2, 4069–4100, 2014

trophic events could be suveyed shortly after their occurrence (Thunell et al., 1999; McHugh et al., 2011; Lorenzoni et al., 2012); the results reinforced the earthquake-induced interpretation proposed for some "homogenite-type" layers (Chapron et al., 1999; Beck et al., 2007).

For historical and older events, the seismic origin of a specific layer can be established:

- directly, using intrinsic characteristics (texture, origin of components, overall geometry, etc., (see references in Beck, 2009, and Beck et al., 2007);

- indirectly, (i) on the basis of correlations with reported seismic events (for historical seismicity) (e.g. Siegenthaler et al., 1987; Piper et al., 1992; Chapron et al., 1999; Beck et al., 2012); (ii) when detecting the same paleo-event in a large area independantly from local setting (e.g. variable slope dip). This second approach is especially used for deep structures, as subduction (e.g.: Gracia et al., 2010; Moernaut, 2011; Pouderoux et al., 2012), but, also in some cases, for surface-reaching major faults (e.g. Goldfinger et al., 2007);

- combining both types of arguments.

Direct relationships between an active structure and earthquake-induced sedimentary events are investigated for active faults reaching a sediment/water interface (sea- or lake-bottom), through high resolution imagery or/and coring. This favourable setting recently permitted detailed analyses of fault activity (offsets, slip rates) through adjacent sedimentation (Carrillo et al., 2006, 2008; Bull et al., 2006; Barnes and Pondard, 2010; Beck et al., 2012). The here-presented work was dedicated to one of these cases: the deep part of the Sea of Marmara (northwestern Turkey) developed along the North-Anatolian Fault.

As the sedimentological tools and approaches we used have been previously published (Sari and Çağatay, 2006; Beck et al., 2007, 2012; Uçarkuş, 2010; Çağatay et al., 2012; Drab et al., 2012; Eriş et al., 2012; Campos et al., 2013) only results (data and interpretations) implying paleoseismological aspects will be envisaged here. Detailed sedimentological aspects may be consulted in the above-mentioned publications.

2 Tectonic context and data acquisition

Being the gateway between the Black Sea and the Aegean Sea, with narrow shallow connections (Fig. 1), the Sea of Marmara has become the focus of paleoenvironmental investigations. In particular, Late Quaternary climatic cycles, and especially associated sea level changes, let a strong sedimentary imprint, in shallow parts as well as in deep basins (Çağatay et al., 2000; Major et al., 2006; Vidal et al., 2010; etc.). Different hypothesis (including catastrophic flooding) have been proposed for the last "re-connection" of the three realms through Bosphorus and Dardanelles (Çanakkale Straits) sills (Ryan et al., 1997, 1999; Aksu et al., 1999; Eriş et al., 2007; etc.). For our purpose, the age of the last non marine-to-marine shift of the Sea of Marmara is a key point, both for the chronological frame of recent seismo-tectonic activity and for the change of volume, composition, and behaviour of re-mobilized sediments (impact of water density and circulation).

2.1 Structural setting and recent seismic activity

The whole circum-Mediterranean areas represent complex and active plate boundaries where subduction and faulting are responsible for high seismic hazards (in Ambraseys, 2009). Among microplates located between the two major Eurasian and African plates, the Anatolian plate (Fig. 1 insert; McClusky et al., 2000; Flerit et al., 2003; Reilinger et al., 2006) is highly investigated as its boundaries have produced catastrophic earthquakes and represent a high permanent seismic risk. More precisely, the northern limit of the Anatolian Plate corresponds to the – right lateral strike slip – North Anatolian Fault (N.A.F. in the following), which northern branch follows the Sea of Marmara from the Izmit Gulf (East) to the Aegean Sea (West) (Barka and Kadinsky-Cade, 1988;

NHESSD
2, 4069–4100, 2014

Armijo et al., 2002; Polonia et al., 2004; McNeill et al., 2004; Gasperini et al., 2011; etc.). Beside the dominant strike slip displacement, the importance of normal faulting and fast subsidence has been underlined, especially for the Central and Çinarcik Basins (Cormier et al., 2006; Carton et al., 2007).

The migration of historical catastrophic ruptures along the N.A.F. has been intensively investigated aiming to understand past and present stress distribution, and to improve seismic risk assessment (Toksöz et al., 1979; Ambraseys and Jackson, 2000; Ambraseys, 2002; Hubert-Ferrari et al., 2002; Altunel et al., 2004; Aksoy et al., 2010; Fraser et al., 2011; Uçarkuş et al., 2011; Meghraoui et al., 2012; etc.). In particular, two destructive ruptured sections have been surveyed (offset and length) respectively West and East of the Sea of Marmara: (1) the M_w 7.4 1912 Ganos event, (2) the M_w 7.4 1999 Izmit event. As the deep basins of the Sea of Marmara are bounded or crosscut by the N.A.F. (Fig. 1), several offshore surveys have been dedicated to analyze its submerged section. Morphological and sedimentary impacts of major recent earthquakes have been searched using: seismic reflection with different resolutions and penetrations, multibeam and side scan sonar, different types of coring, and remote operating vehicles (R.O.V.) (Armijo et al., 2005). The different results concern: (1) deep fluids explusion related to seismo-tectonic activity (Géli et al., 2008; Tary et al., 2012; Burnard et al., 2012; etc.), (2) mass wasting and creep (Zitter et al., 2012; Shillington et al., 2012; (3) deep sedimentation specificities (McHugh et al., 2006; Sari and Çağatay, 2006; Beck et al., 2007; Çağatay et al., 2012; Drab et al., 2012); (4) detection and dating of historical co-seismic scarps (Armijo et al., 2005; Uçarkuş, 2010). Historical tsunamis reports and modelling (Altinok et al., 2011; Hébert et al., 2005) complete these different data, taking into account the fact that these phenomena are not systematically associated to earthquakes (Hornbach et al., 2010). Small size lacustrine basins aligned along the N.A.F. East of Izmit have also been studied for paleosesimicity (Aşar, 2013).

The Sea of Marmara, and especially its deep basins, represents a favorable setting for the search of past seismic activity, and, by mean, an essential data source for regional sesmic hazards estimation (cf. Armijo et al., 2005). In the following, we will focus on the Çinarcik and Central basins' recent sedimentary fills, which we studied aiming: (1) to reconstruct a succession of earthquake-induced sedimentery "events", and, (2) to use part of this succession to analyze the activity of the fault zone corresponding to the southern limit of the "inner" Central Basin (as named by Uçarkuş, 2010).

2.2 Data acquisition and processing

The here-used data were collected during two cruises: (1) the MARMACORE survey (on R/V *Marion-Dufresne*), (2) the MARMARASCARPS survey (on R/V *Atalante*). Three types of cores were retrieved: giant gravity piston cores (CALYPSO device), classical Kullenberg-type cores, and very short cores (35 cm) visually picked using the VICTOR R.O.V.. In parallel, high resolution (3.5 kHz) seismic profiles were acquired, and a complete survey with the VICTOR R.O.V. was dedicated to a high precision multibeam bathymetric survey of different deep scarps (Armijo et al., 2005; Uçarkuş, 2010).The second and third types of cores have been analyzed and yielded paleoseismic information (Uçarkuş, 2010; Drab et al., 2012). A preliminary analysis of 7 Calypso cores (with length ranging from 22 to 37 m) and 3.5 kHz imagery has been achieved (Beck et al., 2007). 3 of them (MD01-2425 in Çinarcik Basin, MD01-2429 and MD01-2431 in Central Basin, location on Fig. 1) were chosen for later detailed laboratory sedimentological analyses on split cores (Eriş et al., 2012, and this work):

- sediment composition: microscopic observations, Carbon and carbonates contents (LOI) XRF profiles in selected portions (AVAATECH instrument); bulk magnetic content (BARTINGTON contact sensor with 5 mm measurement interval);
- layering and texture (grain array):
  - X-Ray pictures (SCOPIX device, Migeon et al., 1998)
  - detailed grain size analysis (MALVERN Mastersizer, 2000): base-to-top paths on binary diagrams for turbidites/homogenites layers (in Beck, 2009; Eriş

et al., 2012); particle shape analysis for silt-clay fraction (SYSMEX FPIA-2100 device);

– Anisotropy of Magnetic Susceptibility profiles (2 cm interval) on selected portions (Campos et al., 2013), completed with Anhysteretic Remanent Magnetization (ARM) and Isothermal Remanent Magnetization (IRM) (AGICO MFK1-FA Kappabridge, SQUID and 2G 760R systems).

The chronology is based on AMS ^{14}C calibrated ages: previously published measurements performed in Woods Hole Oceanographic Institution (NOSAMS facility) (in Beck et al., 2007), and a set of new mesurements performed at CEA-Saclay (CNRS-INSU ARTEMIS facility).

3 Recent sedimentation in the Çinarcick and Central basins of the Sea of Marmara

Cores MD01-2425, -2429, and -2431 (location on Fig. 1) were respectively retrieved at 1215 m, 1230 m, and 1170 m depths, with 31.30 m, 37.30 m, and 26.40 m respective lengths. They respectively represent about 17 kyr, 14 kyr, and 18 kyr BP of continuous deposition. The compositions, layering-types, and the general chronostratigraphy, appear very similar between the three cores, thus we will summarize the results obtained for Core MD01-2425 as a reference. They confirm and complete the investigations previously achieved by Eriş et al. (2012).

3.1 The post-LGM succession in the Çinarcick basin (Core MD01-2425)

Figure 2 summarizes the succession within which, especially in the lower (non marine) part, numerous turbidites, often associated to an overlying homogenite, are intercalated. For this reason, we will describe separately these instantaneous sedimentary "events" and the continuous ("back ground") slow sedimentation. A neat subdivision into two successions appears (see also Eriş et al., 2012): (1) a lower part with a mean

NHESSD
2, 4069–4100, 2014

high sedimentation rate (about 5.4 mm yr^{-1}) due to abundant intercalations of coarser instantaneous terrigenous inputs; (2) an upper part with lower mean sedimentation rate (1.3 mm yr^{-1}) and few coarser intercalations. The limit (discussed hereafter) roughly corresponds to the transition from non marine (only connection with the Black Sea) to marine (connection with Aegean Sea and Black Sea) setting. The whole core corresponds to the Late Glacial–Holocene period.

3.1.1 "Back ground" sedimentation

It is represented in the whole core by a hemipelagic silty–clayey mud. Although the word "hemipelagite" should be restricted to marine/oceanic deposits, we also use it for the non marine succession as, in both cases, it is a mixture of clayey-silty terrigenous fraction (clay minerals, quartz, plagioclase, amphibole, pyroxene, fresh micas, opaques) and planctonic biogenic or bio-induced particles (carbonate and silica: calcareous nanoplankton, Diatoms). Additionnal authigenic particles are locally abundant (sulphides, calcite, aragonite, Mn oxydes).

The bulk carbonate content ranges from 8 to 10 % in the upper marine part; it reaches 16 % at the limit non marine/marine. Organic Matter (weight % dried sediment) ranges from 4 to 6 % in lower part, and 7 to 14 % in the upper part. The highest values characterize the 1380–980 cm so-called "sapropelic" interval. This O.M. enrichment has been previously reported in the different basins of the Sea of Marmara, and in the shallower zone between Tekirdağ and Central basins (Çağatay et al., 2000; Reichel and Halbach, 2007; Beck et al., 2007; Vidal et al., 2010). The different proposed ages are in agreement and a 11-to-7.5 kyr BP period (cal ^{14}C without reservoir correction) can be attributed to this particular episode.

We include into the "background" sediments numerous silty–sandy laminated intervals present in the upper marine part. They are 1 to 3 cm thick and display millimetric parallel planar bedding, involving subtle changes in grain size (up to very fine sand) and mineralogy of detrital components. They have been observed in the three basins

(Tekirdağ, Central, Çinarcik) with same characteristics and occurrence frequency (Beck et al., 2007). We relate these levels to in situ slight reworking by episodic increase of bottom current velocities. A minor part of these intervals (see hereafter) show slow angle micropragradation (flaser bedding type) and are associated to homogenites, thus included into instantaneous gravity reworking events.

3.1.2 Homogenites + turbidites (HmTu) occurrences

Detailed analyses and characterizations of homogenites and their association with turbidites (here labelled HmTu) has been previously published (references in Chapron et al., 1999; Beck et al., 2007; Campos et al., 2013), and their use as paleo-earthquake indicator underlined. They were initially called "seismoturbidites" in Eriş et al. (2012). On split core surface and X-ray pictures, a series of such layers have been visually identified (Fig. 2) mostly in non marine lower part of the core. With up to 1 m thickness, they consist of: (1) a basal coarse layer with overall normal graded bedding, sometimes subdivided into second order graded episodes (similar to classical turbidite lower term), (2) strongly homogenous fine-grained (2 to 8 µm mean grain size) interval, lacking internal variation, and displaying an anomalously high magnetic foliation. As the content and particle shapes of the homogene upper term are identical to what is observed in the hemipelagic mud, the AMS contrast is attributed to a particular grain array (Campos et al., 2013) and, by mean, to a specific settling process. The sharp break between the two terms is often preceeded by a thin interval with flaser bedding-type layering indicating to-and-fro (oscillatory) current, and/or by a specific grain-size evolution. We interpreted this transitional interval as a consequence of oscillation of the whole water mass (seiche effect, reflected tsunami), thus an effect of earthquake and/or massive subaqueous landslide.

In the upper marine part of the succession (Fig. 2), these HmTu "events" are scarce and thinner; they only display a discrete coarser layer and homogene mud with same texture as in the non marine HmTu events. Some classical turbidites were also found in Core MD01-2425. We discarded them in the following, as we could not ensure their earthquake triggering using our criteria; this choice probably minimizes the total number of inferred recorded paleo-earthquakes. The contrast between the two parts of the succession (roughly between Late Glacial and Holocene) is a matter of debate (in Beck et al., 2007). To explain the abundance of terrigenous arrivals in the Late Glacial, we may envisage: either higher storage of sediments in subaqueous deltas and subsequent higher potential for gravity reworking (climatic influence), or more frequent and powerfull earthquakes (tectonic influence)? A change in water density vertical profile and in circulation may also account for the distribution of bedload and suspended load. A similar problem has been underlined for the post-LGM fill of large peri-alpine lakes (Beck et al., 1996).

3.1.3 The non marine to marine transition – age and implications

Due to its importance for the study of the last climatic cycle, the hydrologic evolution of the Sea of Marmara has been intensively surveyed through sedimentation. Biological, chemical, mineralogical, and isotopic proxies, have been analyzed to detect the respective influence of the Black Sea and the Aegean Sea since the Last Glacial Maximum (MIS 2) depending on their surface level (Çağatay et al., 2000; Major et al., 2006; Reichel and Halbach, 2007; Eriş et al., 2007; Vidal et al., 2010). The impact of these variations has also been investigated in shallow parts (Çağatay et al., 2003).

Based on detailed data from cores taken in Central Basin and between Tekirdağ and Central basins, Reichel and Halbach (2007) proposed a modelling of fresh water and marine water mixing. Their results fit with their detection of a calcite peak (30 %) related to authigenic precipitation and interpreted as the result of a first mixing of bottom anoxic fresh water with surface oxic marine water. According to their radiocarbon dating, this changed occurred at 13 cal kyr BP. Vidal et al. (2010) concluded to a slightly different scenario: beginning of Aegean influence at 14.7 kyr cal BP and progressive increase of the mixing, lasting 2 kyr, and followed at 12.8 kyr cal BP by an increased of terrigenous continental organic material. They relate the latter to the beginning of Younger Dryas. The calcite maximum may correspond to the end of mixing process. The end of signif-

NHESSD
2, 4069–4100, 2014

icant Black Sea input at 11.5 kyr cal BP (Vidal et al., 2010) may correspond to the end of the calcite-rich episode. Differences may be due to data sets respectively coming from a deep basin floor (Vidal et al., 2010) and from a shallower setting between two basins (Reichel and Halbach, 2007).

In the here-studied cores, X-ray pictures (Fig. 3 insert) permit to identify a 2 to 5 cm-thick, conspicuous layer of highly bioturbated mud, overlain by about 1 cm of laminated silty mud (parallel planar bedding). It is marked by an increase of fine-grained plant debris, and an abrupt change in magnetic content with respect to hemipelagic intervals. It also corresponds to the last occurrence of Diatoms frustules fragments. A XRF chemical profile (core scanning) performed across this layer – from 40 cm below to 100 cm above – did not display any abrupt change but rather the beginning of a very progressive increase of Br, Mo, and S, considered as diagnostic for more marine environment. According to our measurements, Carbonate content reaches a maximum just below this level (named "reference layer" in the following) and sharply decreases above.

Combining all published results (and our ^{14}C results) we consider our "reference layer"as the Y.D. base and we will use, for the paleo-seismic record discussed hereafter, a 12.8 cal kyr BP age.

3.2 Correlations between Çinarcik and Central Basins and inside Central Basin

In order to extract a paleoseismic record through HmTu events, we checked: (1) a regional correlation between Central and Çinarcik basins (MD01-2425, -2429, and -2431; see also Beck et al., 2007; Eriş et al., 2012); (2) a more localized correlation on both sides of an active scarp in Central Basin (Fig. 4). The catastrophic pre-Late Glacial event (pLGH on Fig. 4) detected on high resolution profiles and cored at Site MD01-2431 (Beck et al., 2007) was not reached at Site MD01-2425.

Figure 3 displays the general correlation on the basis of high resolution bulk Magnetic Susceptibility (MS) profiles. All other measured parameters (not added here: mineralogy and chemistry, biogenic and bio-induced markers), ^{14}C ages, and the non marine-to-marine change horizon, complete the correlation critieria. For the same Late Glacial

NHESSD
2, 4069–4100, 2014

part of the succession (from about 16 kyr BP to the marine/no marine limit (our "reference layer", Figs. 2 and 3)), homogenites + turbidites (HmTu) appear more frequent in Core MD01-2425 (Çinarcik Basin) than in Core MD01-2431 (Central Basin). This difference is also mentionned by Drab et al. (2012) for the last 2.5 kyr BP (marine section), based on short piston core; these authors also proposed several event-by-event correlations and attributions to historical earthquakes.

Despite the X-ray pictures resolution and sampling intervals of the different logs, we could not ensure an "event-by-event" correlation between Çinarcik and Central Basins along the whole non marine section. Conversely, an "event-by-event" correlation within the Central Basin could be proposed for the last 2 kyr preceeding the main hydrologic change (blue rectangles on Fig. 3). Figure 4a and b shows the location of Cores MD01-2429 and MD01-2431 and the overall correlations previously proposed by Beck et al. (2007) and Eriş et al. (2012) based on 3.5 kHz seismic reflection profile.

4 Inferred co-seismic sedimentary events on both sides of the southern scarp of the Central Basin

The two analyzed sites are on both sides of the southern limit of the "inner" Central Basin (Fig. 4a) with a small relative depth difference (50 m at 1200 m b.s.l.). Figure 4b displays their position with respect to a major active fault scarp. Previous preliminar observations of these cores had demonstrated that the high difference of mean sedimentation rates between the two sites (Fig. 4b) was essentially due to the difference of instantaneous sedimentary events thicknesses (Beck et al., 2007).

Assuming the synchroneity of the "reference layer" in the two cores, a detailed analysis was later performed downcore, starting immediately below. For the fine-grained "back ground" sedimentation, because of its hemipelagic-type deposition, the same sedimentation rate was assumed at the two sites. The proposed layer-by-layer correlation (Fig. 5) is based on: (i) precise delimitation of hemipelagic intervals, with same thicknesses, (ii) similarities of subdivisions within HmTu composite layers. The cor-

NHESSD
2, 4069–4100, 2014

rrelation could be achieved for a 2 m succession in Core MD01-2431 which appears equivalent to a 6.2 m succession in Core MD01-2429, the whole for a 2 kyr duration. 11 homogenite + turbidites events (HmTu) account for the difference. For the thickest ones (HmTu A, C, E, H, K) the homogene upper term accounts for about 90 % of the thickness increase in the deeper site. Assuming an earthquake origin for these sedimentary events, and the tendancy of the associated suspension to settle in deepest areas (in Chapron et al., 1999), we consider the increased fills of the downgoing side as successive "seals off" of the created co-seismic scarps (Fig. 6 insert, case 2a). In the Lesser Antilles, Beck et al. (2012) described an active normal fault upon which the sea floor is maintained flat and horizontal, being each co-seismic offset quite exactly compensated by a coeval silty-sandy homogenite (Fig. 6 insert, case 2b). We tentatively applied their 2b model to the Central Basin events. 10 of the 11 events were plot on an age vs. thickness difference log (Fig. 6). 6 of them led to significant values between 40 cm to 160 cm (Fig. 6).

Although the investigated sediments are recent with a reduced depth-in-core, a possible compaction effect has to be discussed as: (i) it concerns mainly clayey-silty material, (ii) the thickness of the homogenite term is up to ten times higher on the hanging wall with respect to the footwall. Based on this differential compaction, a 10 % maximum estimate is thus proposed for a correction of the thickness difference (leading to about 44 to 178 cm).

The inferred offsets were separated by variable time intervals (100 to 550 yr); if taking into account the 11 events, a mean 180 yr interval is deduced. The time distribution is in agreement with previously published paleoseismic results based on sedimentary record in the same area (Beck et al., 2007; Drab et al., 2012). In the present study, a precise rupturing site could be attributed to the sedimentary events.

NHESSD
2, 4069–4100, 2014

5 Discussion

The proposed used of homogenites + turbidites (HmTu) to analyze subaqueous active faulting along the inner Central Basin led to estimate a set of inferred co-seismic offsets, for a 2 kyr-lasting period. As it is a 2-D approach, the results only concern a vertical component (cf. Figs. 4 and 6). The latter may represent either the vertical component of an oblique slip displacement or a subvertical (normal here) one. West of the Central Basin, a historical scarp was observed and analyzed (Armijo et al., 2005; Uçarcuş, 2010) displaying locally low angle dipping slickensides. This site belongs to a NAF section with dominant strike slip behaviour. Applying such low angles displacements to account for our vertical offset values, especially the highest, would result in anomalously high lateral offsets (e.g. 15° dip and 144 cm vertical component). Otherwise, the here-analyzed site is considered as a limit of a pull apart basin (Armijo et al., 2005; Uçarcuş, 2010), and different investigations highlighted the importance of vertical component in Izmit Gulf and Tekirdağ Basin (Cormier et al., 2006; Carton et al., 2007). Based on tsunami modelling applied to the Sea of Marmara, Hébert et al. (2005) conclude to the importance of vertical offset related to faulting or to submarine landslides. In the following, we thus assumed that our estimated values represent dominant vertical throws, i.e. normal offsets.

With respect to an approach in terms of paleo-magnitude (M_w) of the earthquakes associated to estimated offsets, additionnal data are needed to propose an actual, complete, paloseismic approach: horizontal length and lower limit of rupturing. Nevertheless, we propose estimations for two inferred offset values (44 cm and 178 cm; Fig. 6; with compaction effect). We consider:

- a 70° mean fault dip as displayed by deep seismic reflection data from Laigle et al. (2008)
- two possibilities for the sea bottom rupture horizontal length: 8 km if considering the total length of the SW side of the Inner Central Basin "losange", or 5 km if considering only the eastern continuous scarp (see on Fig. 4a)

– a brittle/ductile transition at two different depths following the distribution proposed by Inan et al. (2007, in Uçarkuş, 2010): 12 km and 20 km. These values respectively correspond to the western termination and the eastern half of the analyzed scarp.

We applied the Moment Magitude Calculator software (Jet Propulsion Laboratory and University of Southern Carolina, 2013) with two current shear modulus values. The results (Table 1) show M_w comprised between 5.9 and 6.6. The corresponding M_O (seismic moment) values, the fault length and the fault surface values, were plotted on two diagrams, respectively from Kanamori and Anderson (1975) and Henry and Das (2001). Our results better fit with intraplate earthquakes distribution and using a 8 km rupture length (thus the whole SW limit of the Inner Central Basin).

In terms of paleoseismicity, our results only concern the pre-Holocene period. Regarding the thickness difference between the two sites (three times higher on the hanging wall), there is no drastic change at the non marine/marine limit. For the marine (upper) part, a specific sedimentary processe is still driving an overthickening on the hanging wall ("inner" Central Basin) but not enough to compensate the scarp as before (insert Fig. 6, Holocene situation). The few thin homogenites + turbidites we observed cannot account for the difference. Nevertheless, the top of the marine part (partly disturbed in our giant piston cores) corresponds to a conspicuous increase in M.S. (Fig. 3). A 4 m long piston core, taken close to Site MD01-2429, shows a set of turbidites + homogenites (Drab et al., 2012); the corresponding interval is approximately comprised between 2 kyr BP and Present.

To explain the remaining thickness difference during the 13 kyr BP-to Present period, we favour a hypothesis implying two combined mechanisms: (1) the water vertical density profile led to more hyperpycnal distribution of gravity reworked sediments, (2) coarse material strongly decreased due to change in weathering condition. Checking this hypothesis needs further higher resolution analysis of the sediments (especially the laminated episodes). The present day depth difference between Sites MD01-2429 and MD01-2431 (Fig. 5a and b) – about 50 m – corresponds to about 12.5 kyr. The

NHESSD
2, 4069–4100, 2014

post-"reference layer" interval (the marine part) shows a 20 m "additionnal" thickness, leading to about 70 m of total vertical displacement (approx. 75 m slip with a mean 70° fault plane dip). This could correspond to a 6 mm yr^{-1} mean normal offset, which distribution into creep vs. co-seismic increments has to be further discussed. Considering a relatively low number of sedimentary events in the Central Basin with respect to Tekirdağ Basin, Drab et al. (2012) underlined different explanation, including partial creeping along the Central segment. For a longer period, we observe a similar difference between Central Basin and Çinarcik Basin, with evidences of a specific behaviour of the southern limit of the former.

6 Conclusions

The detailed sedimentological analysis of a sedimentary accumulation bounding a subaqueous active fault confirmed the occurrence of co-seismic offsets through coeval specific events. It permitted to estimate their values and also confirms a dominantly co-seismic behaviour (null or negligible creep) at least for a 2 kyr time interval. With up to 1.8 m normal slip values, added to local structural and seismological data, this archive led to propose paleo-magnitude values (M_w between 5.9 and 6.6) compatible with historical data. These results bring additionnal arguments for seismic hazard assessment along the central portion of the N.A.F. (Sea of Marmara's Central Basin).

Acknowledgements. The presented investigations were possible thanks to CNRS-INSU funding through ISTerre Laboratory and the Universe Sciences Observatory of Grenoble. CNRS-INSU is acknowledged for the access to ARTEMIS national AMS radiocarbon measurement facilities. C. Campos' PhD thesis and stay in ISTerre Laboratory were funded through Venezuela's FUNDAYACUCHO Grant No. 20093262. We thank Anne-Lise Develle (EDYTEM Laboratory) for XRF profiles performing and help for their interpretation.

References

Adams, J.: Paleoseismicity of the Cascadian subduction zone: evidence from turbidites off the Oregon–Washington margin, Tectonics, 9, 569–583, 1990.

Aksoy, M. E., Meghraoui, M., Vallee, M., and Cakir, Z.: Rupture characteristics of the A. D. 1912 Murefte (Ganos) earthquake segment of the North Anatolian fault (western Turkey), Geology, 38, 991–994, doi:10.1130/G13447.1, 2010.

Aksu, A. E., Hiscott, R. N., and Yasar, D.: Oscillating Quaternary water levels of the Marmara Sea and vigorous outflow into the Aegean Sea from the Marmara Sea–Black Sea drainage corridor, Mar. Geol., 153, 275–302, 1999.

Altinok, Y., Alpar, B., Özer, N., and Aykurt, H.: Revision of the tsunami catalogue affecting Turkish coasts and surrounding regions, Nat. Hazards Earth Syst. Sci., 11, 273–291, doi:10.5194/nhess-11-273-2011, 2011.

Altunel, E., Meghraoui, M., Akyüz, H. S., and Dikbas, A.: Characteristics of the 1912 coseismic rupture along the North Anatolian Fault Zone (Turkey): implications for the expected Marmara earthquake, Terra Nova, 16, 198–204, 2004.

Ambraseys, N. N.: The seismic activity in the Marmara Sea region over the last 704 years, B. Seismol. Soc. Am., 92, 1–18, 2002.

Ambraseys, N. N.: Earthquakes in the Mediterranean and Middle East: a Multidisciplinary Study of Seismicity up to 1900, Cambridge University Press, Cambridge, UK, 947 pp., 2009.

Ambraseys, N. N. and Jackson, J. A.: Seismicity of the Sea of Marmara (Turkey) since 1500, Geophys. J. Int., 141, F1–F6, 2000.

Armijo, R., Meyer, B., Navarro, S., King, G. C. P., and Barka, A. A.: Asymmetric slip partitioning in the Sea of Marmara pull-apart: a clue to propagation processes of the North Anatolian Fault?, Terra Nova, 14, 80–86, 2002.

Armijo, R., Pondard, N., Meyer, B., Uçarkus, G., Mercier de Lépinay, B., Malavieille, J., Dominguez, S., Gutscher, M.-A., Schmidt, S., Beck, C., Çagatay, N., Çakir, Z., Imren, C., Eriş, K., Natalin, B., Özalaybey, S., Tolun, L., Lefèvre, I., Seeber, L., Gasperini, L., Rangin, C., Emre, O., and Sarikavak, K.: Submarine fault scarps in the Sea of Marmara pull-apart (North Anatolian Fault): implications for seismic hazard in Istanbul, Geochem. Geophy. Geosy., 6, Q06009, doi:10.1029/2004GC000896, 2005.

Aşar, U.: Lacustrine Paleoseismic Records from the North Anatolian Fault, Turkey, Ph.D. thesis memoir, University of Ghent, 209 pp., 2013.

Barka, A. A. and Kadinsky-Cade, K.: Strike-slip fault geometry in Turkey and its influence on earthquake activity, Tectonics, 7, 663–684, 1988.
Barnes, P. M. and Pondard, N.: Derivation of direct on-fault submarine paleoearthquake records from high-resolution seismic reflection profiles: Wairau Fault, New Zealand, Geochem. Geophy. Geosy., 11, Q11013, doi:10.1029/2010GC003254, 2010.
Beck, C.: Late Quaternary lacustrine paleo-seismic archives in north-western Alps: examples of earthquake-origin assessment of sedimentary disturbances, Earth-Sci. Rev., 96, 327–344, 2009.
Beck, C., Manalt, F., Chapron, E., Van Rensbergen, P., and De Batist, M.: Enhanced seismicity in early post-glacial period: evidences from the posy-Würm sediments of Lake Annecy, northwestern Alps, J. Geodyn., 22, 155–171, 1996.
Beck, C., Mercier de Lépinay, B., Schneider, J.-L., Cremer, M., Çağatay, N., Wendenbaum, E., Boutareaud, S., Ménot, G., Schmidt, S., Weber, O., Eris, K., Armijo, R., Meyer, B., Pondard, N., Gutscher, M.-A., the MARMACORE Cruise Party, Turon, J.-L., Labeyrie, L., Cortijo, E., Gallet, Y., Bouquerel, H., Gorur, N., Gervais, A., Castera, M.-H., Londeix, L., de Rességuier, A., and Jaouen, A.: Late Quaternary co-seismic sedimentation in the Sea of Marmara's deep basins, in: Sedimentary Records of Catastrophic Events, edited by: Bourrouilh-Le Jan, F., Beck, C., and Gorsline, D., Special Issue, Sediment. Geol., 199, 65–89, 2007.
Beck, C., Reyss, J.-L., Leclerc, F., Moreno, E., Feuillet, N., Barrier, L., Beauducel, F., Boudon, G., Clément, V., Deplus, C., Gallou, N., Lebrun, J.-F., Le Friant, A., Nercessian, A., Paterne, M., Pichot, T., and Vidal, C.: Identification of deep subaqueous co-seismic scarps through specific coeval sedimentation in Lesser Antilles: implication for seismic hazard, Nat. Hazards Earth Syst. Sci., 12, 1755–1767, doi:10.5194/nhess-12-1755-2012, 2012.
Burnard, P., Bourlange, S., Henry, P., Géli, L., Tryon, M. D., Natalin, B., Sengör, A. M. C., Özeren, M. S., and Çağatay, M. N.: Constraints on fluid origins and migratin velocities along the Marmara Main Fault (Sea of Marmara, Turkey) using helium isotopes, Earth Planet. Sc. Lett., 341, 68–78, 2012.
Bull, J. M., Barnes, P. M., Lamarche, G., Sanderson, D. J., Cowie, P., Taylor, S. K., and Dix, J. K.: High-resolution record of displacement accumulation on an active normal fault: implications for models of slip accumulation during repeated earthquakes, J. Struct. Geol., 28, 1146–1166, 2006.

Çağatay, M. N., Görür, N., Algan, O., Eastoe, C., Tchapalyga, A., Ongan, D., Kuhn, T., and Kuşçu, I.: Late Glacial–Holocene palaeoceanography of the Sea of Marmara: timing of connections with the Mediterranean and the Black Seas, Mar. Geol., 167, 191–206, 2000.
Çağatay, M. N., Görür, N., Polonia, A., Demirbağ, E., Sakinç, M., Cormier, M.-H., Capotondi, L., McHugh, C., Emre, Ö., and Eriş, K.: Sea level changes and depositional environments in the İzmit Gulf, eastern Marmara Sea, during the Late Glacial–Holocene period, Mar. Geol., 202, 159–173, 2003.
Çağatay, N., Erel, L., Bellucci, L. G., Polonia, A., Gasperini, L., Eriş, K. K., Sancar, Ü., Biltekin, D., Uçarkuş, G., Ulgen, Ü. B., and Damci, E.: Sedimentary earthquake records in the Ýzmit Gulf, Sea of Marmara, Turkey, Sediment. Geol., 282, 347–359, 2012.
Campos, C., Beck, C., Crouzet, C., Demory, F., Van Welden, A., and Eris, K.: Deciphering hemipelagites from homogenites through Magnetic Susceptibility Anisotropy – paleoseismic implications (Sea of Marmara and Gulf of Corinth), Sediment. Geol., 292, 1–14, 2013.
Carrillo, E., Audemard, F., Beck, C., Cousin, M., Jouanne, F., Cano, V., Castilla, R., Melo, L., and Villemin, T.: A Late Pleistocene natural seismograph along the Boconò Fault (Mérida Andes, Venezuela): the moraine-dammed Los Zerpa palæo-lake, Bulletin of the French Geological Society, 177, 3–17, 2006.
Carrillo, E., Beck, C., Audemard, F. A., Moreno, E., and Ollarves, R.: Disentangling Late Quaternary climatic and seismo-tectonic controls on Lake Mucubají sedimentation (Mérida Andes, Venezuela) in: Lake Systems: Sedimentary Archives of Climate Change and Tectonic, edited by: De Batist, M. and Chapron, E., Palaeogeogr. Palaeocl., 259, 284–300, 2008.
Carton, H., Sing, S. C., Hirn, A., Bazin, S., de Voogd, B., Vigner, A., Ricolleau, A., Cetin, S., Oçakoğlu, N., Karakoç, F., and Sevilgen, V.: Seismic imaging of the three-dimensional architecture of the Çinarcik Basin along the North Anatolian Fault, J. Geophys. Res., 112, B060101, 1–17, doi:10.1029/2006JB00548, 2007.
Chapron, E., Beck, C., Pourchet, M., and Deconinck, J.-F.: 1822 earthquake-triggered homogenite in Lake Le Bourget (NW Alps), Terra Nova, 11, 86–92, 1999.
Cormier, M.-H., Seeber, L., McHugh, C. M. G., Polonia, A., Çağatay, M. N., Emre, O., Gasperini, L., Görür, N., Bortoluzzi, G., Bonatti, E., Ryan, W. B. F., and Newman, K. R.: The North Anatolian fault in the Gulf of Izmit (Turkey): rapid vertical motion in response to minor bends of a non-vertical continental transform, J. Geophys. Res., 111, B04102, doi:10.1029/2005JB003633, 2006.

NHESSD
2, 4069–4100, 2014

Estimation of successive co-seismic vertical offsets

C. Beck et al.

Drab, L., Hubert Ferrari, A., Schmidt, S., and Martinez, P.: The earthquake sedimentary record in the western part of the Sea of Marmara, Turkey, Nat. Hazards Earth Syst. Sci., 12, 1235–1254, doi:10.5194/nhess-12-1235-2012, 2012.

Eriş, K., Ryan, W. B. F., Çağatay, N., Sancar, U., Lericolais, G., Menot, G., and Bard, E.: The timing and evolution of the post-glacial transgression across the Sea of Marmara shelf south of Istanbul, Mar. Geol., 243, 57–76, 2007.

Eriş, K., Çağatay, N., Beck, C., Mercier de Lepinay, B., and Campos, C.: Late-Pleistocene to Holocene sedimentary fills of the Çınarcık Basin of the Sea of Marmara, Sediment. Geol., 281, 151–165, 2012.

Flerit, F., Armijo, R., King, G. C. P., Meyer, B., and Barka, E.: Slip partitioning in the Sea of Marmara pull-apart determined from GPS velocity vectors, Geophys. J. Int., 154, 1–7, 2003.

Fraser, J., Vanneste, K., and Hubert-Ferrari, A.: Recent behaviour of the North Anatolian Fault: insights from an integrated paleoseismological data set, J. Geophys. Res., 115, 1–27, doi:10.1029/JB006982, 2010.

Gasperini, L., Polonia, A., Çağatay, M. N., Bortoluzzi, G., and Ferrante, V.: Geological slip rates along the North Anatolian Fault in the Marmara Sea, Tectonics, 30, TC6001, doi:10.1029/2011TC002906, 2011.

Géli, L., Henry, P., Andre, C., Zitter, T., Çağatay, N., Mercier de Lepinay, B., LePichon, X., Sengor, A. M. D., Gorur, N., Natalin, B., Ucarkus, G., Ozeren, S., Volker, D., Gasperini, L., Bourlanger, S., and the MarNaut Scientific Party: Gas emissions and active tectonics within the submerged section of the North Anatolia Fault zone in the Sea of Marmara, Earth Planet. Sc. Lett., 274, 34–39, 2008.

Gracia, E., Vizcaino, A., Escutia, C., Asioi, A., Rodes, A., Pallas, R., Garcia-Orellana, Lebreiro, J., S., and Goldfinger, C.: Holocene earthquake record offshore Portugal (SW Iberia): testing turbidite paleoseismology in a slow-convergence margin, Quaternary Sci. Rev., 29, 1156–1172, 2010.

Goldfinger, C., Morey, A. E., Nelson, C. H., Gutierez-Pastor, J., Johnson, J. E., Karabanov, E., Eriksson, A., and shipboard scientific party: Rupture lengths and temporal history of significant earthquakes on the offshore and north coast segments of the Northern San Andreas Fault based on turbidite stratigraphy, Earth Planet. Sc. Lett., 254, 9–27, 2007.

Hébert, H., Schindelé, F., Altinok, Y., Alpar, B., and Gazioglu, C.: Tsunami hazard in the Marmara Sea (Turkey): a numerical approach to discuss active faulting and impact on the Istanbul coastal areas, Mar. Geol., 215, 23–43, 2005.

NHESSD

2, 4069–4100, 2014

Estimation of successive co-seismic vertical offsets

C. Beck et al.

Henry, C. and Das, S.: Aftershocks of large shallow earthquakes: faults dimensions, aftershock area expansion and scaling relations, Geophys. J. Int., 147, 272–293, 2001.
Hornbach, M. J., Braudy, N., Briggs, R. W., Cormier, M.-H., Davis, M. B., Diebold, J. B., Dieudonne, N., Douilly, R., Frohlich, C., Gulick, S. P. S., Johnson, H. E., Mann, P., McHugh, C. M. G., Ryan-Mishkin, K., Prentice, C. S., Seeber, L., Sorlien, C. C., Steckler, M. S., Symithe, S. J., Taylor, F. W., and Templeton, J.: High tsunami frequency as a result of combined strike-slip faulting and coastal landslides, Nat. Geosci., 3, 783–788, 2010.
Hubert-Ferrari, A. I., Armijo, R., King, G., Meyer, B., and Barka, A.: Morphology, displacement, and slip rates along the North Anatolian Fault, Turkey. J. Geophys. Res., 107, ETG 9-1-ETG 9-33+, doi:10.1029/2001JB000393, 2002.
Jet Propulsion Laboratory and University of Southern Carolina: Moment Magnitude Calculator, available at: http://quakesim.org/tools/moment-magnitude-calculator, 2013.
Kanamori, H. and Anderson, D. L.: Theoritical basis of some empirical relations in seismology, B. Seismol. Soc. Am., 65, 1073–1095, 1975.
Ken-Tor, R., Agnon, A., Enzel, Y., and Stein, M.: High-resolution geological record of historic earthquakes in the Dead Sea basin, J. Geophys. Res., 106, 2221–2234, 2001.
Laigle, M., Becel, A., de Voogd, B. A., Hirn, A., Taymaz, T., and Ozalaybey, S.: A first deep seismic survey in the Sea of Marmara: deep basins and whole crust architecture and evolution, Earth Planet. Sc. Lett., 270, 168–179, 2008.
Lorenzoni, L., Benitez-Nelson, C. R., Thunell, R. C., Hollander, D., Varelan, R., Astor, Y., Audemard, F. A., and Muller-Karger, F. E.: Potential role of event-driven sediment transport on sediment accumulation in the Cariaco Basin, Venezuela, Mar. Geol., 307, 105–110, doi:10.1016/j.margeo.2011.12.009, 2012.
Major, C., Goldstein, S. L., Ryan, W. B. F., Lericolais, G., Piotrowski, A. M., and Hajdas, I.: The co-evolution of Black Sea level and composition through the last deglaciation and its paleoclimatic significance, Quaternary Sci. Rev., 25, 2031–2047, 2006.
Marco, S. and Agnon, A.: Prehistoric earthquake deformations near Masada, Dead Sea graben, Geology, 23, 695–698, 1995.
McCalpin, J. M.: Paleoseismology, vol. 45, International Geophysics Series, Academic Press, 798 pp., 2009.
McNeill, L. C., Mille, A., Minshull, T. A., Bull, J. M., Kenyon, N. H., and Ivanov, M.: Extension of the North Anatolian Fault into the North Aegean Trough: evidence for transtension,

strain partitioning, and analogues for Sea of Marmara basin models, Tectonics, 3, 1–12, doi:10.1029/2002TC001490, 2004.
McClusky, S., Bassalanian, S., Barka, A., Demir, C., Ergintav, S., Georgiev, I., Gurkan, O., Hamburger, M., Hurst, K., Hans-Gert, H.-G., Karstens, K., Kekelidze, G., King, R., Kotzev, V., Lenk, O., Mahmoud, S., Mishin, A., Nadariya, M., Ouzounis, A., Paradissis, D., Peter, Y., Prilepin, M., Reilinger, R., Sanli, I., Seeger, H., Tealeb, A., Toksöz, M. N., and Veis, G.: Global positioning system constraints on plate kinematics and dynamics in the eastern Mediterranean and Caucasus, J. Geophys. Res., 105, 5695–5719, 2000.
McHugh, C. M. G., Seeber, L., Cormier, M.-H., Dutton, J., Cagatay, N., Polonia, A., Ryan, W. B. F., and Gorur, N.: Submarine earthquake geology along the North Anatolia fault in the Marmara Sea, Turkey: a model for transform basin sedimentation, Earth Planet. Sc. Lett., 248, 661–684, doi:10.1016/j.epsl.2006.05.038, 2006.
McHugh, C., Seeber, L., Braudy, N., Cormier, M.-H., Davis, M. B., Diebold, J. B., Dieudonne, N., Douilly, R., Gulick, S. P. S., Hornbach, M. J., Johnson III, H. E., Ryan Miskin, K., Sorlien, C., Steckler, M., Symithe, S. J., and Templeton, J.: Offshore sedimentary effects of the 12 January 2010 Haiti earthquake, Geology, 39, 723–726; doi:10.1130/G31815.1, 2011.
Meghraoui, M., Aksoy, M. E., Akyuz, H. S., Ferry, M., Dikbas, A., and Altunnel, E.: Paleoseismology of the North Anatolia Fault at Guzelkoy (Ganos segment, Turkey): size and recurrence time of earthquake ruptures west of the Sea of Marmara, Geochem. Geophy. Geosy., 13, 1–26, 2012.
Migeon, S., Weber, O., Faugères, J. C., Saint Paul, J.: A new X-ray imaging system for core analysis, Geo-Mar. Lett., 18, 251–255, 1998.
Moernaut, J.: Sublacustrine Landslide Processes and their Paleoseismological Significance: Revealing the Recurrence Rate of Giant Earthquakes in South-Central Chile, Ph.D. thesis, University of Ghent, 274 pp., 2011.
Moretti, M., Alfaro, P., Caselles, O., and Canas, J. A.: Modelling seismites with a digital shaking table, Tectonophysics, 304, 369–383, 1999.
Piper, D. J. W., Cochonat, P., Ollier, G., Le Drezen, E., Morrison, M, and Baltzer, A.: Evolution progressive d'un glissement rotationnel en un courant de turbidité: cas du séisme de 1929 des Grands Bancs (Terre Neuve), CR Acad. Sci. Série II, 314, 1057–1064, 1992.
Polonia, A., Gasperini, L., Amorosi, A., Bonatti, E., Bortoluzzi, G., Çağatay, M. N., Capotondi, L., Cormier, M.-H., Görür, N., McHugh, C. M. G., and Seeber, L.: Holocene slip rate of the North Anatolian Fault beneath the Sea of Marmara, Earth Planet. Sc. Lett., 227, 411–426, 2004.

NHESSD
2, 4069–4100, 2014

Estimation of successive co-seismic vertical offsets

C. Beck et al.

Pouderoux, H., Lamarche, G., and Proust, J.-N.: Building an 18 000-year-long paleo-earthquake record from detailed deep-sea turbidite characterisation in Poverty Bay, New Zealand, Nat. Hazards Earth Syst. Sci., 12, 2077–2101, doi:10.5194/nhess-12-2077-2012, 2012.
Rangin, C., Demirbag, E., Imren, C., Crusson, A., Normand, A., Le Drezen, E., and Le Bot, A.: Marine Atlas of the Sea of Marmara (Turkey), IFREMER/GENAVIR, 2001.
Reichel, T. and Halbach, P.: An authigenic calcite layer in the sediments of the Sea of Marmara, a geochemical marker horizon with paleoceanographic significance, Deep-Sea Res. Pt. II, 54, 1201–1215, 2007.
Reilinger, R. E., McClusky, S., Vernant, P., Lawrence, S., Ergintav, S., Cakmak, R., Ozener, H., Kadirov, F., Guliev, I., Stepanyan, R., Nadariya, M., Hahubia, G., Mahmoud, S., Sakr, K., Ar-Rajehi, A., Paradissis, D., Al-Aydrus, A., Prilepin, M., Guseva, T., Evren, E., Dmitrotsa, A., Filikov, S. V., Gomez, F., Al-Ghazzi, R., and Karam, G.: GPS constraints on continental deformation in the Africa–Arabia–Eurasia continental collision zone and implications for the dynamics of plate interactions, J. Geophys. Res., 111, B05411, 1–26, doi:10.1029/2005JB004051, 2006.
Rodriguez-Pascua, M. A., Calvo, J. P., De Vicente, G., and Gòmez-Gras, D.: Soft-sediment deformation structures interpreted as seismites in lacustrine sediments of the Prebetic Zone, SE Spain, and their potential use as indicators of earthquake magnitudes during the Late Miocene, Sediment. Geol., 135, 117–135, 2002.
Rodriguez-Pascua, M. A., De Vicente, G., Calvo, J. P., and Perez-Lopez, R.: Similarities between recent seismic activity and paleoseismites during the late Miocene in the external Betic Chain (Spain): relationship by the *b* value and the fractal dimension, J. Struct. Geol., 25, 749–763, 2003.
Ryan, W. B. F. and Pitman III, W. C.: Noah's Flood. The New Scientific Discoveries About Events that Changed History, Toutchstone Book, Simon & Schuster, New York, 1999.
Ryan, W. B. F., Pitman III, W. C., Major, C. O., Shimkus, K., Moskalenko, V., Jones, G. A., Dimitrov, P., Gorür, N., Sakinc, M., and Yüce, H.: An abrupt drowning of the Black Sea shelf, Mar. Geol., 138, 119–126, 1997.
Sari, E. and Çağatay, M. N.: Turbidites and their association with past earthquakes in the deep Cinarcik Basin of the Marmara Sea, Geo-Mar. Lett., 26, 69–76, 2006.
Shillington, D. J., Seeber, L., Sorlien, C. C., Steckler, M. S., Kurt, H., Dondurur, D., Cifici, G., Imren, C., Cormier, M.-H., McHugh, C. M. G., Gurcay, S., Poyraz, D., Okay, S., Atgin, O., and

NHESSD
2, 4069–4100, 2014

Estimation of successive co-seismic vertical offsets

C. Beck et al.

Diebold, B.: Evidence for widespread creep on the flanks of the Sea of Marmara transform basin from marine geophysical data, Geology, 40, 439–442, doi:10.1130/G32652.1, 2012.
Siegenthaler, C., Finger, W., Kelts, K., and Wang, S.: Earthquake and seiche deposits in Lake Lucerne, Switzerland, Eclogae Geol. Helv., 80, 241–260, 1987.
Strasser, M., Anselmetti, F. S., Fäh, D., Giardini, D., and Schnellmann, M.: Magnitudes and source areas of large prehistoric northern Alpine earthquakes revealed by slope failures in lakes, Geology, 34, 1005–1008, 2006.
Tary, J. B., Géli, L., Guennou, C., Henry, P., Sultan, N., Cagatay, N., and Vidal, V.: Microevents produced by gas migration and expulsion at the seabed: a study based on sea bottom recordings from the Sea of Marmara, Geophys. J. Int., 190, 993–1007, 2012.
Thunell, R., Tappa, E., Valera, R., Llano, M., Astor, Y., Muller-Karger, F., and Bohrer, R.: Increased marine sediment suspension and fluxes following an earthquake, Nature, 398, 233–236, 1999.
Toksöz, M. N., Shakal, A. F., and Michael, A. J.: Space-time migration of earthquakes along the North Anatolian fault zone and seismicity gaps, Pure Appl. Geophys., 924, 1258–1270, 1979.
Uçarkuş, G.: Active Faulting and Earthquake Scarps along the North-Anatilian Fault in the Sea of Marmara, Ph.D. thesis, ITU, Eurasian Institute of Earth Sciences, Istanbul, 173 pp., 2010.
Uçarkuş, G., Çakır, Z., and Armijo, R.: Western termination of the Mw 7.4, 1999 Izmit earthquake rupture: implications for the expected large earthquake in the Sea of Marmara, Turk. J. Earth Sci., doi:10.3906/yer-0911-72, 2011.
Vidal, L., Menot, G., Joly, C., Bruneton, H., Rostek, F., Çağatay, N., Major, C., and Bard, E.: Hydrology in the Sea of Marmara during the last 23 ka: implications for timing of Black Sea connections and sapropel deposition, Paleoceanography, 25, PA1205, doi:10.1029/2009PA001735, 2010.
Wetzler, N., Marco, S., and Heifetz, E.: Quantitative analysis of shear-induced turbulence in lake sediments, Geology, 38, 303–306, 2010.
Zitter, T., Grall, C., Henry, P., Özeren, M. S., Çağatay, M. N., Şengor, A. M. C., Gasperini, L., Mercier de Lépinay, B., and Géli, L.: Distribution, morphology and triggers of submarine mass wasting in the Sea of Marmara, Mar. Geol., 329, 58–74, 2012.

Table 1. Estimation of moment magnitudes M_w for the southwestern scarp of the Central Basin.

			Horizontal	rupture length
		brittle/ductile limit	5 km	8 km
3.0 1011 dyne cm^{-2}	47 cm	12 km	5.9 M_w	6.1 M_w
shear modulus	offset	20 km	6.1 M_w	6.2 M_w
2.5 1011 dyne cm^{-2}	47 cm	12 km	5.9 M_w	6.0 M_w
shear modulus	offset	20 km	6.0 M_w	6.1 M_w
3.0 1011 dyne cm^{-2}	190 cm	12 km	6.3 M_w	6.5 M_w
shear modulus	offset	20 km	6.5 M_w	6.6 M_w
2.5 1011 dyne cm^{-2}	190 cm	12 km	6.3 M_w	6.4 M_w
shear modulus	offset	20 km	6.4 M_w	6.6 M_w

NHESSD
2, 4069–4100, 2014

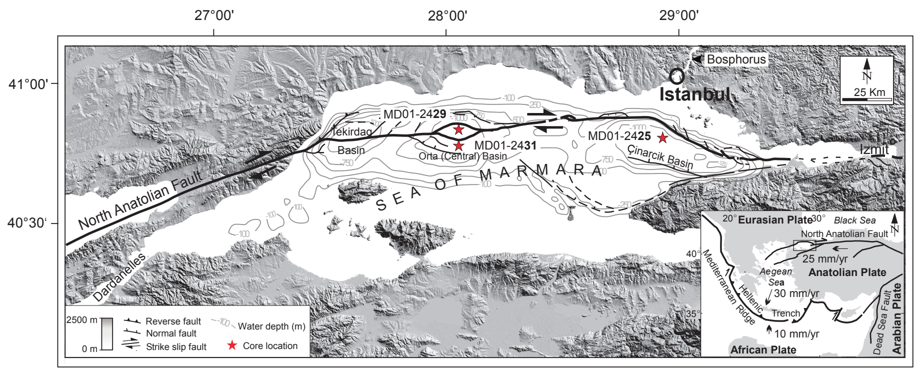

Figure 1. The Sea of Marmara and the North Anatolian Fault: simplified bathymetry and active structures. Location of analyzed core. NAF geometry simplified from Armijo et al. (2002, 2005); GPS kinematics from McClusky et al. (2000), Reilinger et al. (2006).

NHESSD
2, 4069–4100, 2014

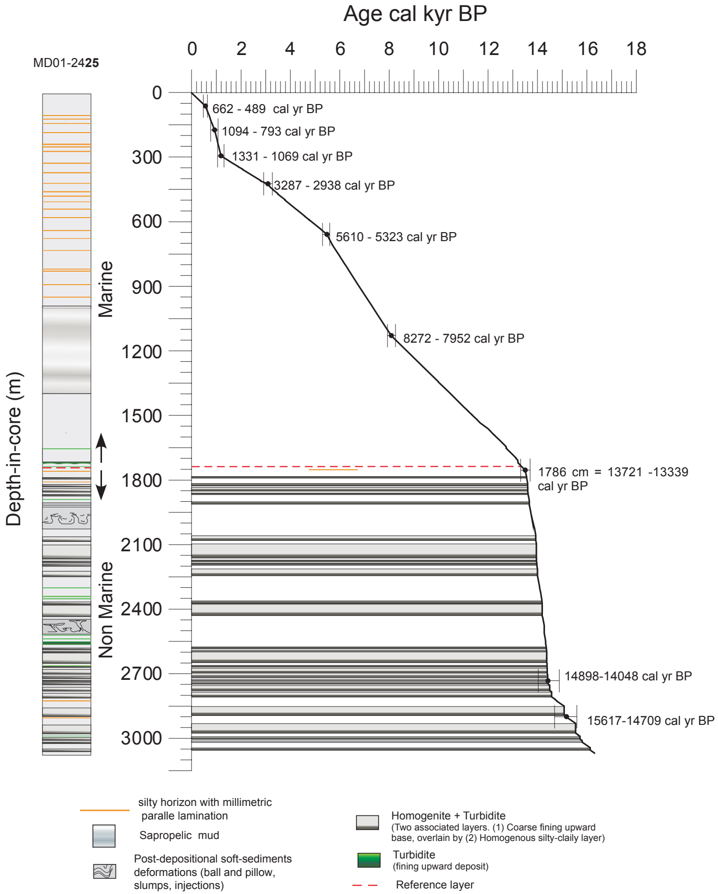

Figure 2. Age/depth curve of Core MD01-2425 (Çinarcik Basin) displaying major instantaneous deposits (homogenite + turbidite). Red dashed line indicates the limit between non marine (below) and marine sequences (reference layer displayed on Figs. 3 and 5); pLGH: pre-Late Glacial Homogenite (Beck et al., 2007).

NHESSD
2, 4069–4100, 2014

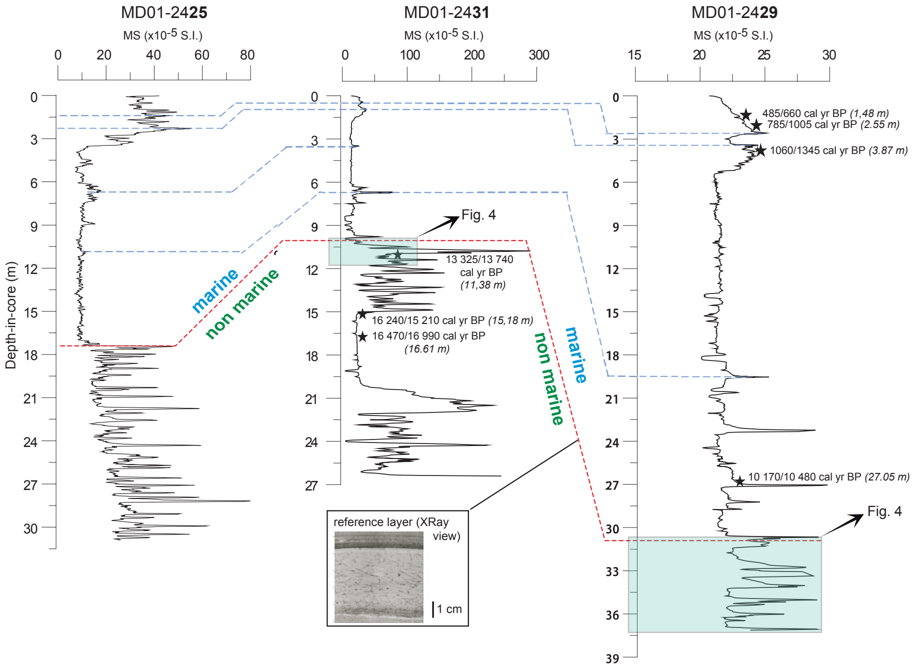

Figure 3. Chronostratigraphic correlations between the Çinarcik Basin (Core MD01-2425) and the Central Basin (Cores MD01-2429 an -2431). Blue rectangles correspond to close up and detailed correlation on Fig. 5.

NHESSD
2, 4069–4100, 2014

Estimation of successive co-seismic vertical offsets

C. Beck et al.

Title Page
Abstract | Introduction
Conclusions | References
Tables | Figures
◀| |▶
◀ ▶
Back | Close
Full Screen / Esc
Printer-friendly Version
Interactive Discussion

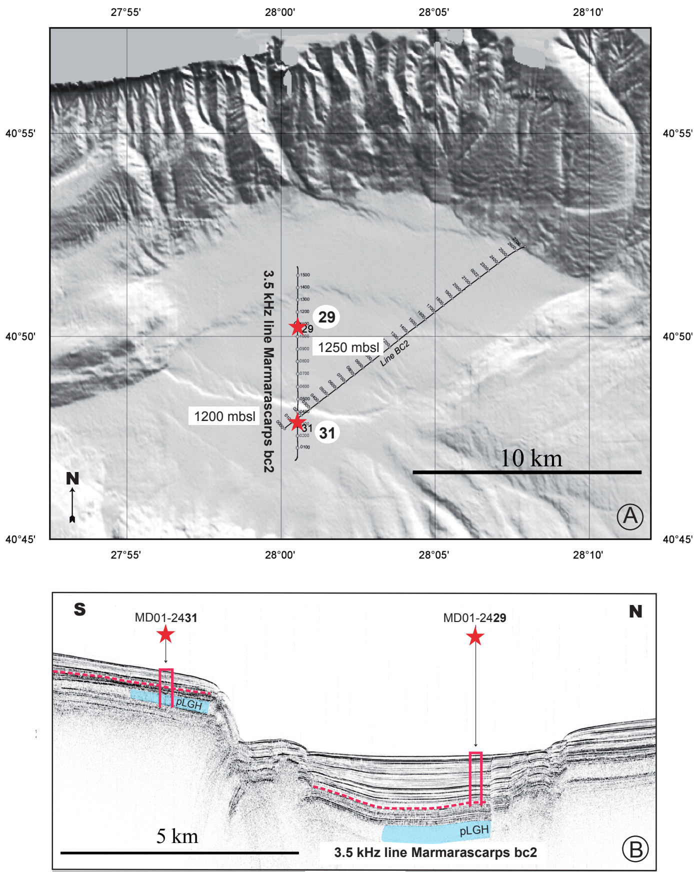

Figure 4. Detailed location of Orta/Central Basin's long cores. **(A)** Bathymetry taken from Rangin et al. (2001); **(B)** very high resolution seismic profile from MARMARASCARPS survey (Armijo et al., 2005; Uçarkuş, 2010). Red dashed line indicates the limit between non marine (below) and marine sequences (also underlined on Figs. 3–5).

NHESSD
2, 4069–4100, 2014

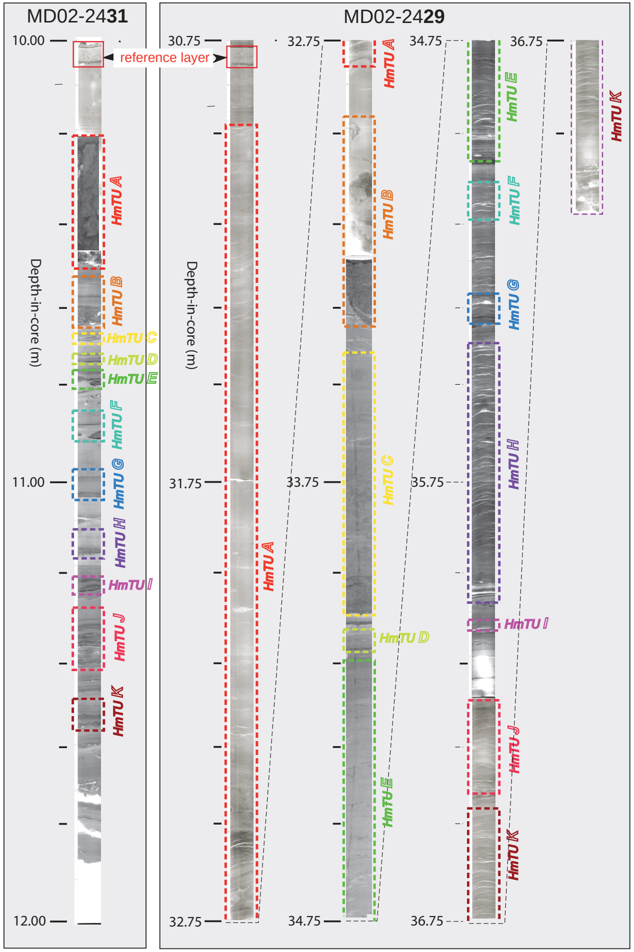

Figure 5. X-ray close up of two synchronous portions of Cores MD01-2429 and MD01-2431, displaying individually correlated sedimentary events (homogenite + turbidite).

NHESSD
2, 4069–4100, 2014

Estimation of successive co-seismic vertical offsets

C. Beck et al.

Title Page
Abstract Introduction
Conclusions References
Tables Figures
◀I ▶I
◀ ▶
Back Close
Full Screen / Esc
Printer-friendly Version
Interactive Discussion

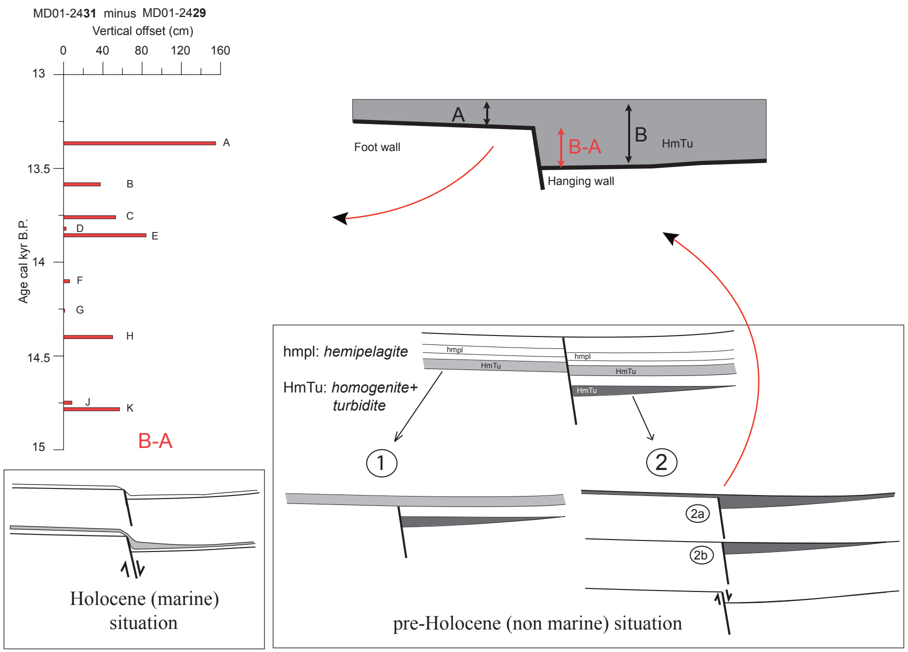

Figure 6. Successive inferred individual co-seismic offsets deduced from homogenites + turbidites (HmTu) thickness differences (insert sketch modified from Beck et al., 2012).

NHESSD
2, 4069–4100, 2014

Estimation of successive co-seismic vertical offsets

C. Beck et al.

Title Page
Abstract | Introduction
Conclusions | References
Tables | Figures
◄◄ | ►►
◄ | ►
Back | Close
Full Screen / Esc
Printer-friendly Version
Interactive Discussion